See page 1754

Treatment of Brain Inflammatory Diseases by Delivering Exosome Encapsulated Anti-inflammatory Drugs From the Nasal Region to the Brain

Xiaoying Zhuang[1,2], Xiaoyu Xiang[2], William Grizzle[3], Dongmei Sun[4], Shuangqin Zhang[4], Robert C Axtell[5], Songwen Ju[2], Jiangyao Mu[2], Lifeng Zhang[2], Lawrence Steinman[5], Donald Miller[2] and Huang-Ge Zhang[2,6]

[1]College of Veterinary Medicine, Yangzhou University, Jiangsu, China; [2]James Graham Brown Cancer Center, Department of Microbiology and Immunology, University of Louisville, Louisville, Kentucky, USA; [3]Department of Pathology, University of Alabama at Birmingham, Birmingham, Alabama, USA; [4]Department of Medicine, University of Alabama at Birmingham, Birmingham, Alabama, USA; [5]Department of Neurology and Neurological Sciences, Stanford University School of Medicine, Stanford, California, USA; [6]Louisville Veterans Administration Medical Center, Louisville, Kentucky, USA

In this study, exosomes used to encapsulate curcumin (Exo-cur) or a signal transducer and activator of transcription 3 (Stat3) inhibitor, *i.e.*, JSI124 (Exo-JSI124) were delivered noninvasively to microglia cells via an intranasal route. The results generated from three inflammation-mediated disease models, *i.e.*, a lipopolysaccharide (LPS)-induced brain inflammation model, experimental autoimmune encephalitis and a GL26 brain tumor model, showed that mice treated intranasally with Exo-cur or Exo-JSI124 are protected from LPS-induced brain inflammation, the progression of myelin oligodendrocyte glycoprotein (MOG) peptide induced experimental autoimmune encephalomyelitis (EAE), and had significantly delayed brain tumor growth in the GL26 tumor model. Intranasal administration of Exo-cur or Exo-JSI124 led to rapid delivery of exosome encapsulated drug to the brain that was selectively taken up by microglial cells, and subsequently induced apoptosis of microglial cells. Our results demonstrate that this strategy may provide a noninvasive and novel therapeutic approach for treating brain inflammatory-related diseases.

Received 4 March 2011; accepted 10 July 2011; published online 13 September 2011. doi:10.1038/mt.2011.164

INTRODUCTION

Despite the development of drugs that preferentially target inflammatory cells without harming normal tissues, delivery of these drugs to the brain remains a major challenge because of difficulty in penetrating the blood–brain barrier.[1–4] Hence, further development of many therapeutic agents may have been abandoned because sufficient drug levels in the brain could not be achieved via the systemic circulation. Microglial cells, brain resident macrophages, play a crucial role in many brain inflammatory-related diseases of the central nervous system (CNS) such as schizophrenia, meningitis, migraine headaches, Parkinson's disease, Alzheimer's disease, and brain tumors.[5–8] Although intranasal delivery provides a practical, noninvasive method for delivering therapeutic agents to the brain, the quantities of drug administered nasally that have been shown to be transported directly from nose-to-brain is very low.[9–13] We have previously shown that exosomes are selectively taken up by immature myeloid cells including macrophages.[14] Exosome encapsulated curcumin leads to significantly increased solubility, stability, and bioavailability of the encapsulated curcumin. In this study, we were particularly interested in testing the intranasal delivery of curcumin or a signal transducer and activator of transcription 3 (Stat3) inhibitor to brain microglial cells through the use of exosomes. We tested the hypothesis that intranasal delivery of the curcumin or Stat3 inhibitor, JSI-124 (cucurbitacin I), would allow the compounds to reach brain microglial cells and inhibit lipopolysaccharide (LPS) induced microglial cell activation, delay experimental autoimmune encephalomyelitis (EAE) disease, and inhibit tumor growth *in vivo*. Our results suggest that intranasal delivery of anti-inflammatory agents, such as curcumin and JSI-124 provides a promising noninvasive approach for the treatment of brain inflammatory-related diseases such as glioblastoma and EAE.

RESULTS

Intranasally administered exosomes are rapidly transported to the brains of mice

To determine whether exosomes can be transported intranasally into the brain, we administered Odyssey 800 dye-labeled exosomes into nontumor-bearing mice. Odyssey 800 dye-labeled exosomes (10 μg/10 μl) isolated from different types of cells (**Figure 1a**) were administered using a small pipette as five doses in alternating sides of the nose as 2-μl drops spaced 2 minutes apart. Mice were killed 30 minutes after intranasal delivery and their brains

Correspondence: *Huang-Ge Zhang, James Graham Brown Cancer Center, Department of Microbiology and Immunology, University of Louisville, CTRB 309, 505 Hancock Street, Louisville, Kentucky 40202, USA. E-mail: h0zhan17@louisville.edu*

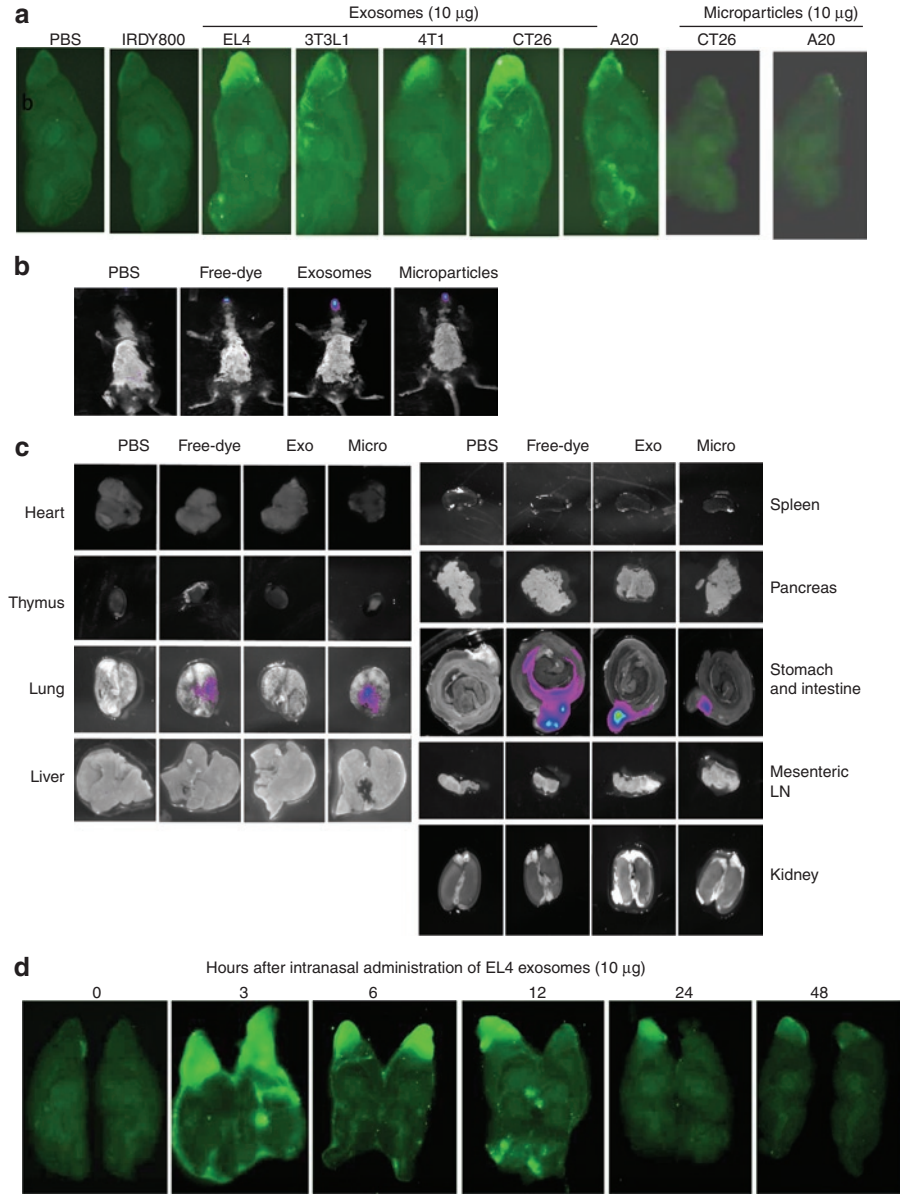

Figure 1 Intranasal administration of exosomes results in localization to the brain. A total of 10 μg of IRDye 800-labeled exosomes (green) released from different types of cells as listed or DIR dye-labeled EL-4 exosomes (**b**,**c**) were administered intranasally into C57BL/6j mice. (**a**) 30 minutes or at different time points (**d**) postintranasal administration, the brain was cut sagittally, and the ventral sides of cut brain were placed against the scanner for imaging using the (**a**,**d**) Odyssey laser-scanning imager or (**b**) whole mice or (**c**) each organ were imaged using the Carestream Molecular Imaging System. Representative sagittal images from the center of the brain ($n = 5$; **a**,**d**), images of whole body (**b**), or images of each organ ($n = 5$; **c**) are shown. Results were obtained from three independent experiments with five mice in each group of mice.

were examined for the presence of the exosomes using an Odyssey scanner. Fluorescent labeled exosomes were observed as being diffusely located in the brain with their primary location being in the olfactory bulb, suggesting that translocation of exosomes to the brain occurred rapidly (**Figure 1a**). In contrast, no microparticles (500 nm–1 μm) larger than exosomes (30–100 nm)[15] were detected in the brain (**Figure 1a**). Very little or no fluorescence was detected in the brain of mice intranasally administered phosphate-buffered saline (PBS) or free dye (**Figure 1a**). These results suggest that particle size is a critical factor for translocation from the nasal region to the brain. No apparent toxicity or behavioral abnormalities were observed in any of the mice during and after (30 days) the experiment. To further determine whether the exosomes intranasally administered also traffick to other tissues, whole mice (**Figure 1b**) and most of the organs (**Figure 1c**) from the mice having been intranasally administered exosomes were imaged. Three hours after intranasal administration of DIR-dye labeled EL-4 exosomes the mice were imaged (the reason for using DIR dye, instead of IRDye800 dye, was to avoid the auto fluorescent interference generated in the intestine). The imaging results indicate that in addition to exosomes that were located in the brain, significant amounts of exosomes were located in the intestines but were not found in other organs tested (**Figure 1b,c**). Interestingly, most of the microparticles went to the lung and

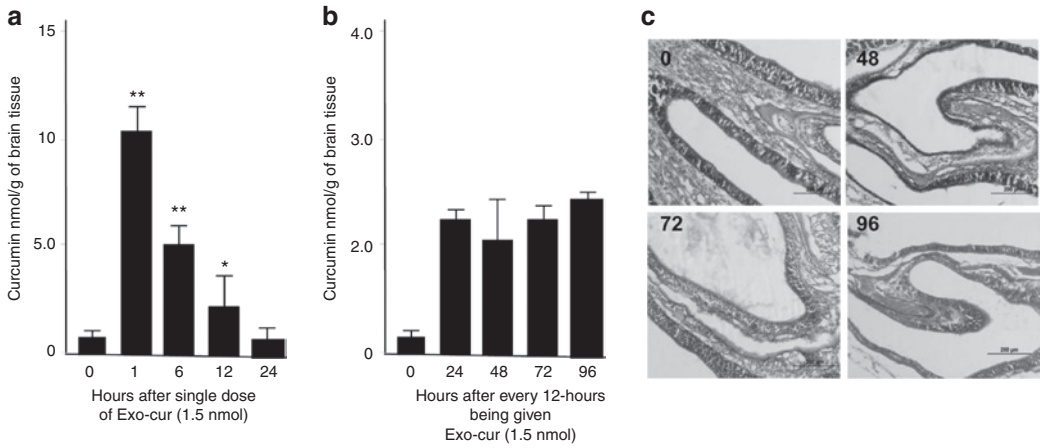

Figure 2 Repeated intranasal administration of Exo-cur maintains bioavailability of curcumin in the brain. C57BL/6j mice were administered (**a**) intranasally once or (**b**) repeatedly every 12 hours with 1.5 nmol curcumin or Exo-cur. Brains of mice from each group (n = 5) at each time point were removed at the time indicated in **a** and **b** after intranasal administration, and curcumin was extracted from the tissue using a method as described.[14] The concentration of curcumin in extracts was determined by high-performance liquid chromatography (HPLC) as described in the Materials and Methods section. Standard deviation (±s.d.) is presented as error bars. $^{**}P < 0.01$. (**c**) Hematoxylin and eosin (HE) stained nasal tissues collected at different time points after mice having been treated with Exo-cur. Original magnification ×10.

intestine (**Figure 1b,c**). Similar distribution patterns of intranasally administered exosomes were observed in mice in a LPS-induced inflammation condition (data not shown). We next investigated distribution of intranasal IRDye800-labeled exosomes in the brain at various times after intranasal delivery of EL-4 exosomes. Mice were given 10 µg IRDye800-labeled EL-4 T cell derived exosomes over a 10-minute time period as noted above, and then killed 3 to 48 hours later. Fluorescence was stronger throughout the brain 3 hours after intranasal delivery (**Figure 1d**). Fluorescence remained visible at the olfactory bulb region of the brain 24 hours after delivery. The animals did not exhibit any apparent toxicities or behavioral abnormalities during and after the course of this experiment.

Next, we determined the capacity of exosomes to deliver curcumin to the brain. Quantification of curcumin intranasally delivered by EL-4 exosomes (Exo-cur) indicated that the curcumin reached peak concentrations 1 hour after intranasal administration, and was still detectable in the olfactory bulb region within the first 12 hours after a single intranasal administration of Exo-cur (**Figure 2a**). Repeated administration of Exo-cur every 12 hours maintained the curcumin concentration at an average of 2.6 ± 0.4 nmol/g of brain tissue (**Figure 2b**). Collectively, these data suggest that exosomes can be used as a novel noninvasive vehicle for delivery of drugs to the brain. We observed no visible abnormality of the nasal mucosal epithelial structure after repeated intranasal administration of Exo-cur (**Figure 2c**), no loss of body weight, and no visible changes in the fecal contents (data not shown).

Intranasally delivered exosomes are taken up by microglial cells

To further identify specific targeting of cells by exosomes, *in vivo* biodistribution of fluorescent dye PKH26-labeled EL-4 exosomes was conducted. Double fluorescence PKH26$^+$Iba-1$^+$ positive cells (Iba-1 is a specific marker for microglial cells) were visible in brain microglial cells 15 minutes after intranasal delivery of exosomes

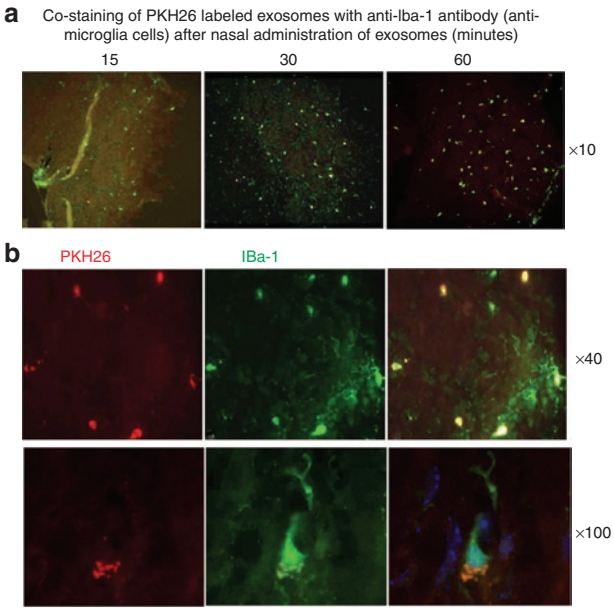

Figure 3 Exosomes administered intranasally are taken up by microglial cells. A total of 10 µg of PKH26-labeled EL-4 exosomes (red) were administered intranasally to C57BL/6j mice. (**a**) Mice were sacrificed 15, 30, and 60 minutes after intranasal administration of PKH26-labeled EL-4 exosomes. Brain tissue sections were fixed as described in the Materials and Methods section. Frozen sections (30 µm) of the anterior part of the brain were stained with the antimicroglial cell marker Iba-1 (green color). Slides were examined and photographed through an upright microscope with an attached camera (Olympus America, Center Valley, PA). Representative photographs of brain sections of mice having been intranasally administered PKH26-labeled exosomes for varying times (**a**) or 60 min at low (×40) and high (×100) magnification are shown (**b**). Each photograph is representative of three different independent experiments (n = 5). Original magnifications ×10, ×40, and ×100.

(**Figure 3a**). Within an hour after injection, >60% of the Iba-1$^+$ microglial cells were PKH26$^+$ (**Figure 3a,b**), suggesting that the injected exosomes were taken up by the microglial cells.

Exosome encapsulated curcumin inhibits LPS-induced brain inflammation and myelin oligodendrocyte glycoprotein (MOG) induced autoimmune responses in an EAE model

Microglial cells have been shown to play a crucial role in brain inflammation. To determine whether the exosomes are functioning as a delivery vehicle to carry anti-inflammatory drugs, such as curcumin, and therefore treat brain inflammatory diseases, two independent disease models were tested. In the first model, intranasal administration of exosome encapsulated curcumin was used for treating LPS-challenged mice. Based on fluorescence-activated cell sorting (FACS) analysis the results indicate that 2 hours after LPS challenge, the number of activated inflammatory microglial cells ($CD45.2^{+}IL\text{-}1\beta^{+}$) was reduced significantly in the brain of mice that were treated intranasally with Exo-cur in comparison to the other treatments listed in **Figure 4a**. The reduction of interleukin (IL)-1β in CD45.2 microglial cells was further confirmed by real-time PCR (**Figure 4b**). Further FACS analysis showed that exosomes were taken up by brain macrophages (**Figure 4c**, left panel) including activated ($F4/80^{+}MHCII^{+}$) and nonactivated ones

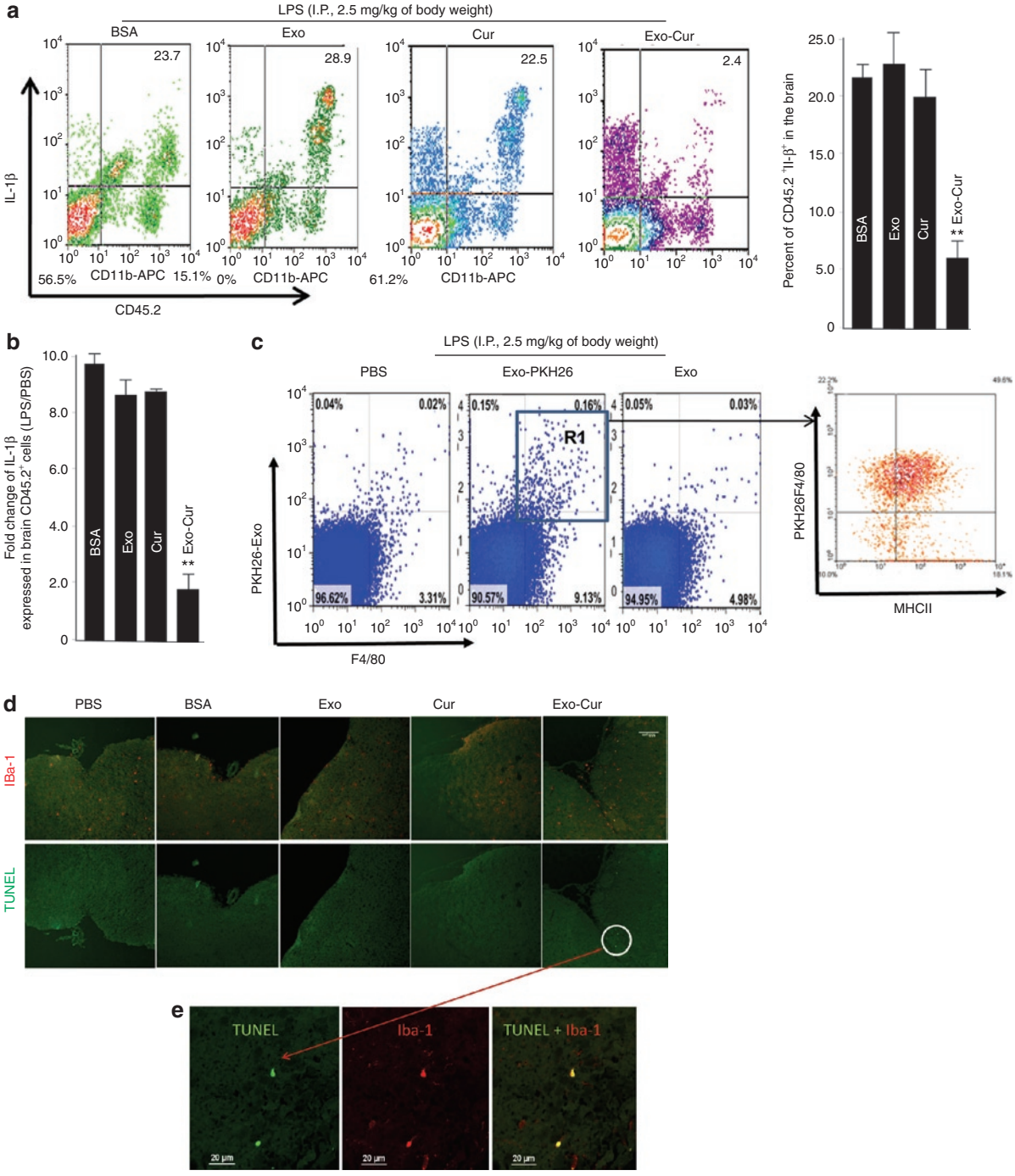

Figure 4 Continued on next page

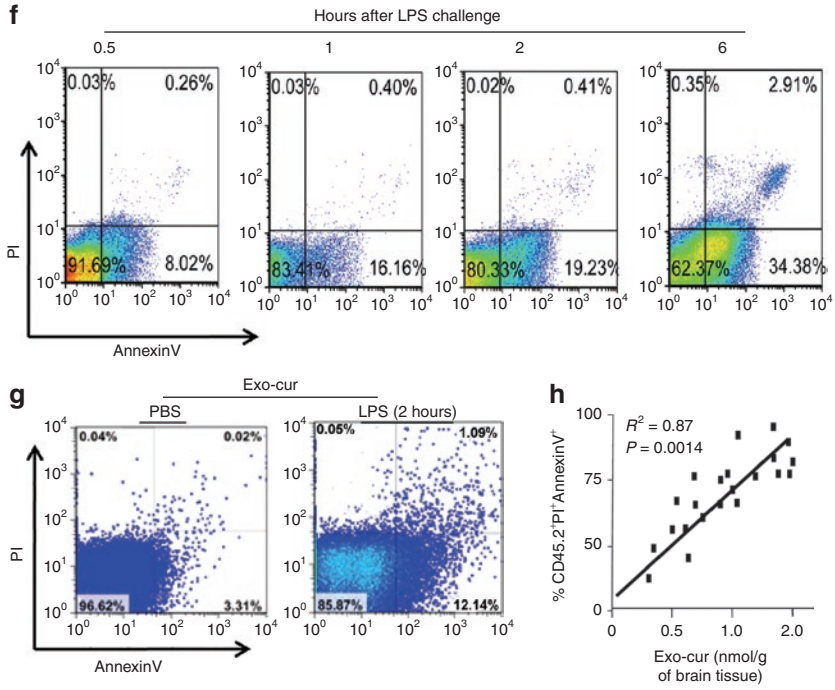

Figure 4 Intranasal administration of Exo-cur leads to induction of apoptosis of the CD45.2$^+$IL-1β$^+$ cell population in lipopolysaccharide (LPS)-induced inflammation. Exo-cur (1.5 nmol/mouse) or control agents as listed in (**a**) were administered intranasally immediately after C57BL/6j mice were intraperitoneally (i.p.) injected with bacterial lipopolysaccharide (2.5 mg/kg). At 2 hours after LPS injection, mice were killed, and the leukocytes in the brains were isolated. The percentage of CD45.2$^+$IL-1β$^+$ cells (**a**) in brain leukocytes was determined by FACS analysis (**a**, left). The percentage of CD45.2$^+$IL-1β$^+$ cells in total brain leukocytes is shown (**a**, histogram graph). Total RNA extracted from FACS sorted CD45.2$^+$ brain cells was used for real-time PCR. Quantitative real-time PCR expression analyses of IL-1β were carried out on CD45.2$^+$ brain cells isolated from mice treated with different agents as listed in **b**. Fold changes in mRNA expression of IL-1β between LPS challenged and nonchallenged controls were determined as described in the Materials and Methods section. Results represent the mean ± s.e.m. of three independent experiments (**b**). A total of 10 µg of PKH26-labeled or unlabeled EL-4 exosomes was administered intranasally to C57BL/6j mice after C57BL/6j mice were i.p. injected with bacterial lipopolysaccharide (2.5 mg/kg); PBS was used as a control. Mice were sacrificed 2 hours after intranasal administration for FACS analysis of PKH26$^+$F4/80$^+$ cells (**c**, left panel) or within the gated R1 region, MHCII$^+$ cells were further determined (**c**, right graph). The brains of mice treated as described in **a** were collected and 30-µm thick frozen sections of the anterior part adjacent to the olfactory bulb of the brain of mice were stained with the antimicroglial cell marker Iba-1 (green color) and stained using a TUNEL staining kit (Roche). Sections were examined by fluorescence microscopy. Representative TUNEL stained brain sections from each group of mice were then photographed at ×10 (**d**) or for Exo-cur treated groups were TUNEL and anti-Iba1 stained and viewed at a magnification of ×60 (**e**). Brain leukocytes were isolated from B6 mice at 0.5, 1, 2, and 6 hours after intranasal administration of Exo-cur (1.5 nmol/mouse) (**f**) or from B6 mice which had been ip injected with LPS (2.5 mg/kg) or PBS for 2 hours before given Exo-cur (**g**). The cells were stained and analyzed for apoptosis (PI$^+$AnnexinV$^+$). Representative FACS analysis results of PI$^+$AnnexinV$^+$ staining is shown in (**f**,**g**). The correlation between the percent of PI$^+$AnnexinV$^+$ and amount of curcumin detected in the brain was calculated using linear regression analysis (**h**).

(F4/80$^+$MHCII$^-$) in the gated R1 region (**Figure 4c**, right panel). The results of TUNEL staining of brain tissue suggested that Exo-cur treatment led to an increase in the number of apoptotic cells in mice administered Exo-cur intranasally (**Figure 4d**). Costaining with a microglial cell-specific antibody (Iba-1 clone) (**Figures 4e**) indicated that double positive cells (TUNEL$^+$IBA-1$^+$) were microglial cells. The induction of apoptosis was further confirmed by the results of FACS analysis (**Figure 4f**). To further confirm that induction of apoptosis is relevant to LPS challenge, and not due to spontaneously induced apoptosis by unidentified factors, percentages of apoptotic leukocytes isolated from Exo-cur treated mice challenged with LPS or PBS as a control was determined. The FACS analysis data suggest that negligible numbers of brain leukocytes of mice challenged with PBS were PI$^+$AnnexinV$^+$ in comparison with mice 2 hours postchallenged with LPS (**Figure 4g**). The induction of apoptotic leukocytes is also correlated with the concentration of curcumin detected in the brain of mice treated with Exo-cur (**Figure 4h**). Collectively, these data support that Exo-cur treatment induces apoptosis in microglial cells of mice challenged with LPS. Because nasal administration of exosomes in this LPS-induced inflammation model (data not shown) did not alter the distribution of exosomes when compared to control mice, *i.e.*, no LPS challenge (**Figure 1**), the biological effects of exosomes on other organs were not further investigated.

To further determine whether intranasal delivery of Exo-cur could prevent inflammation related brain autoimmune disease, MOG-induced EAE in mice was conducted. EAE was induced in 6-week-old female C57BL/6 mice by immunization with MOG35-55 as described previously.[16] Exo-cur was administered intranasally daily for 31 days using the protocol described above and was initiated on day 4 after immunization with the MOG peptide. The mice were sacrificed at day 35 postimmunization. Disease severity was scored based on the method as described previously.[16] The score of PBS, exosomes only, or curcumin only groups of EAE mice was 3.83 ± 0.22, 3.70 ± 0.31, and 3.60 ± 0.12, respectively. The disease severity in Exo-cur-treated mice was significantly reduced

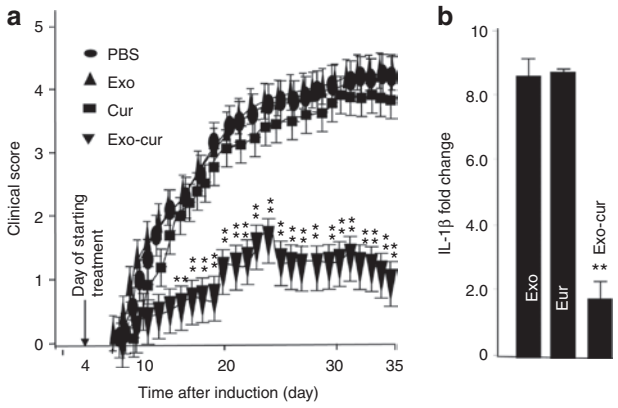

Figure 5 Exosomal curcumin treatment delays and attenuates experimental autoimmune encephalomyelitis (EAE). (**a**) Clinical EAE scores comparing controls with Exo-cur-treated mice. Exo-cur treatment delays and ameliorates EAE. One representative experiment of two independent experiments is shown (n = 10 females per group; mean ± s.e.m.). $^{**}P < 0.01$. (**b**) C57BL/6j mice were immunized with MOG35-55 peptide using procedures described in the Materials and Methods section. Ten days postimmunization, total RNA extracted from FACS sorted CD45.2$^+$ brain cells was used for real-time PCR. Quantitative real-time PCR expression analyses of IL-1β were carried out on CD45.2$^+$ brain cells isolated from mice treated with different agents as listed in **b**. Fold changes in mRNA expression of IL-1β between a PBS control and other groups were determined as described in the Materials and Methods section. Results represent the mean ± s.e.m. of three independent experiments (**b**).

with a maximal disease severity score of 1.53 ± 0.41 (**Figure 5a**). Real-time PCR analysis also demonstrated that the expression of IL-1β in CD45.2 microglial cells was decreased significantly in the Exo-cur treated mice (**Figure 5b**) in comparison with control groups.

Intranasal delivery of an exosome encapsulated Stat3 inhibitor inhibits GL26 tumor growth

Stat3 is activated constitutively in many types of human cancers and plays a critical role in tumor growth including glioblastoma. Microglial cells, the resident macrophages of the brain, have been known to play a critical role in the progression of brain glioblastoma. Therefore, we treated groups of mice bearing intracerebral tumors with exosome encapsulated Stat3 inhibitor JSI-124 (12.5 pmol/10 µl) or exosomes only, JSI-124 only, or PBS as controls. Mice were treated every other day for 15 days beginning on day 3 after tumor cells were implanted. The amount of JSI-124 administered was based on the lack of any evidence of toxicity or behavioral abnormalities in the mice. Imaging data showed a statistically significant decrease in brain-associated photons in Exo-JSI124-treated mice when compared to controls (**Figure 6a**), and was determined on day 9 after tumor cells were injected. Survival times of PBS-, exosomes- or JSI124-control animals ranged from 20 to 30 days. In contrast, Exo-JSI124 treatment significantly prolonged the survival of mice on the average of 44.5 days ($P <$ 0.011) (**Figure 6b**). Moreover, 2 of the 10 Exo-JSI124 treated mice were alive and showed no neurological symptoms at day 90 when they were killed. There was no evidence of tumor at the original implantation site in these two mice. None of the Exo-JSI124-treated animals exhibited evidence of toxicity or behavioral abnormalities during and after the 15-day treatment period. To further investigate if the observed effect was due to inhibition of Stat3 activity in the Exo-JSI124 targeted cells in the brain, the activity of Stat3 in brain CD45.2$^+$ cells was quantitatively determined by western blot analysis based on the detection of pStat3. The results suggest that Exo-JSI124 treatment led to the selective reduction of pStat3 in CD45.2$^+$ microglial cells (**Figure 6c**). The reduction of Stat3 was also correlated with a decrease in the expression of both IL-1β and IL-6 in CD45.2$^+$ microglial cells (**Figure 6d**). Collectively, these data support the idea that Exo-JSI124 is selectively taken up by microglial cells and subsequently inhibits the expression of inflammatory cytokines such as IL-1β and IL-6. We further determined whether intranasal administration of Exo-JSI124 has a direct effect on tumor. The results of hematoxylin and eosin stained brain tumor tissue suggest that tumor adjacent to the olfactory region aggressively invaded the adjacent tissue of mice treated with BSA, Exo, and JSI124. In contrast, mice intranasally administered Exo-JSI124 was characterized as having much less invasiveness (**Figure 6e**). TUNEL staining of the same tumor blots suggest that more TUNEL stained cells, *i.e.*, apoptotic, are detected (**Figure 6f**).

DISCUSSION

The blood–brain barrier has been an insurmountable obstacle to the development of CNS therapeutics, impeding clinical use of otherwise promising therapeutic agents in the treatment of many brain neuron disorders where inflammation plays a causative role. The present study examined a novel approach for intranasal delivery of anti-inflammatory agents to the brain. Our results clearly indicate that anti-inflammatory agents like curcumin or JSI124 are effectively delivered to the brain by exosomes without observable side effects. Furthermore, we have identified microglial cells as being preferentially targeted by exosomes. The successful delivery and therapeutic effects of curcumin or JSI124 loaded exosomes was demonstrated in three independent mouse models, *i.e.*, a LPS-induced brain inflammation model, MOG-induced EAE autoimmune disease, and a GL26 implanted brain tumor model. Microglial cells are well-known to play an essential role in many inflammatory-related brain diseases. The accumulation of myeloid or microglial cells in the brain has been implicated in the promotion of brain tumor growth and progression of brain autoimmune diseases, such as EAE in mouse models and in humans.[17–28] In this study, we found that intranasal administration of Exo-cur led to a significant reduction in the number of microglial cells and that Exo-JSI124 resulted in the enhancement of tumor apoptosis and a concomitant reduction in disease progression in all three models we tested. These findings are also consistent with our results published recently[14] showing that inflammatory cells, such as CD11b$^+$Gr-1$^+$ cells, can be deleted specifically by curcumin encapsulated in exosomes. We demonstrated that mice treated with Exo-cur are protected completely against LPS-induced septic shock[14] and that the protective mechanism is associated with the ability of the Exo-cur to specifically target myeloid cells. Therefore, our strategy of delivering exosome-encapsulated drugs to the brain via intranasal administration could potentially improve the direct delivery of drugs to the CNS with the advantages of target specificity and administration in a noninvasive manner. Our data show that curcumin encapsulated in exosomes not only targets to

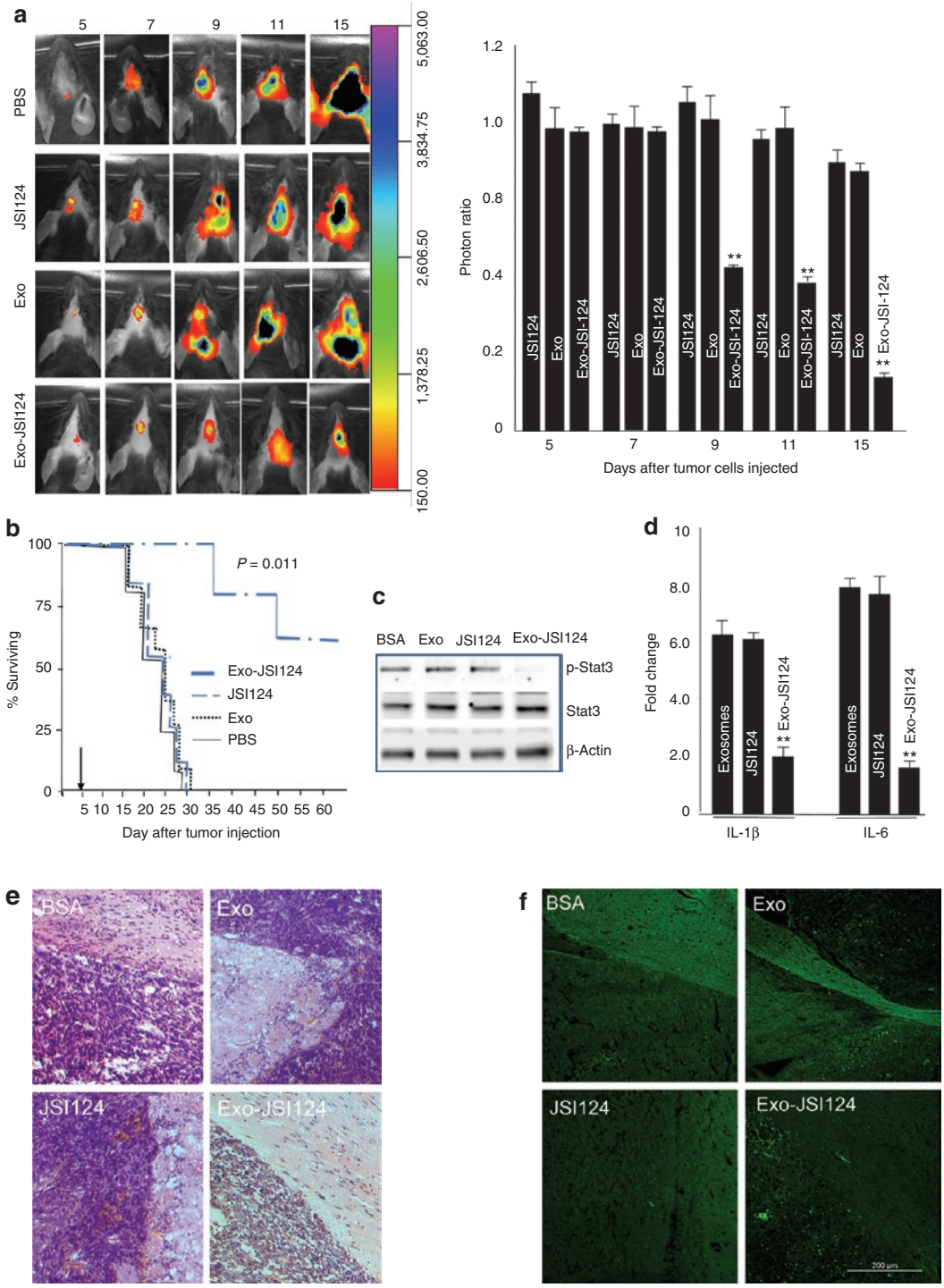

Figure 6 Exosomal JSI124 treatment prevents the growth of *in vivo* injected brain tumor cells. 2×10^4 GL26 cells per mouse were injected intracranially in 6-week-old wild-type B6 mice. Three-day tumor-bearing mice were then treated intranasally on a daily basis with Exo-JSI24, or JSI124 or Exo in PBS or PBS-control for 12 days. The mice were imaged on the postinjection days as indicated in **a**. A representative photograph of brain tumor signals of a mouse from each group ($n = 5$) is shown (**a**; left). The growth potential of injected GL26-Luc cells was determined by dividing photon emissions of mice treated with PBS by the photon emissions of mice treated with JSI124, Exo, or Exo-JSI124 (**a**; right). The results are based on two independent experiments with data pooled for mice in each experiment ($n = 5$) and are presented as the mean ± s.e.m.; $^{**}P < 0.0.1$. (**b**) Percent of Exo-JSI124-treated mice surviving was compared to control mice. One representative experiment of 2 independent experiments is shown ($n = 5$ females per group). Arrows represent days when treatments were started. (**c**) A total of 40 μg of protein or (**d**) RNA extracted from FACS sorted CD45.2$^+$ brain cells from 9 day tumor-bearing mice were used for (**c**) western blot and (**d**) real-time PCR analyses for expression of IL-1β and IL-6. Fold changes in mRNA expression of IL-1β and IL-6 between treated and PBS controls was determined as described in the Materials and Methods section. Results represent the mean ± s.e.m. of three independent experiments (**c**,**d**). Results of hematoxylin and eosin (HE) staining (**e**), or TUNEL staining (**f**) of brain tumor sections and adjacent area of mice treated with the agents listed. Original magnification ×20. Data represent at least three experiments with five mice/group.

inflammatory cells, *i.e.*, microglial cells, but reaches the CNS in sufficient quantity by this route to be effective. Therefore, these results could generate interest in previously abandoned drug compounds and enable an entirely novel approach to CNS drug delivery.

In this study, we also showed that EL-4 exosomes from T cell lines are taken up by microglial cells (~60%) as well as nonmicroglial cells (~40%). Further FACS analysis suggests that both $MHCII^{dim}$ and $MHCII^{high}$ microglial cells can take up exosomes after mice are injected with LPS. These data suggest that both "resting" and "activated" macrophages may take up exosomes. Recently, it has been reported that resting microglial cells preferentially take up exosomes released from oligodendrocytes.[29] We currently do not know whether the discrepancy between the data we generated and that reported by Fritzner *et al*. is due to the source of exosomes or different microenvironmental factors (an in vitro cultured microglial model that Fritzner used versus our intranasal administered exosomes in this study). We believe our data reflects what takes place from the point of using exosomes as a therapeutic delivery vehicle. We speculate that exosomes taken up by naive microglial cells may lead to the induction of immune tolerance in the naive microglial cells to antigens released from the cells producing the exosomes whereas the exosomes taken up by activated microglial cells may lead to activate immune cells. Whether EL-4 exosomes taken up by activated versus naive microglial cells lead to immune tolerance or immune responsiveness to EL-4 exosomal antigens needs to be evaluated in the future.

Although our data presented in this study show that Exo-cur-mediated induction of apoptosis is one of the mechanisms underlying the therapeutic effects, other mechanisms cannot be excluded as curcumin is a pleiotropic agent that can target multiple pathways. Curcumin is also a powerful anti-inflammatory agent with chemopreventive and anticancer properties[30–36] that modulates numerous targets including inhibition of IL-17 induction[37] in different types of cells. Further detailed analysis of the mechanism(s) of action is critical for optimization of curcumin-based therapy, and identification of potential side effects. In addition, we observed that apoptotic cells detected by TUNEL staining are induced as early as 2 hours after Exo-cur treatment. The TUNEL assay usually detects apoptotic DNA fragment degradation that takes place in the latter stages of apoptosis. Whether the early cellular DNA degradation is a unique property of the Exo-cur complex in comparison with free curcumin induced apoptosis we are unsure and this finding needs to be further investigated. Also, since microglial cells are not the only cells targeted by exosomes, the biological effects of other cells, particularly, immune cells infiltrating the brain, including NK cells or $CD11b^{+}Gr\text{-}1^{+}$ myeloid cells, needs to be further studied.

Our results indicate that direct intranasal-to-brain transport is feasible. In our initial distribution study, we found rapid movement of exosomes into the brain within 1 hour of intranasal administration. This finding is consistent with the extraneuronal pathway that has been proposed for transport of therapeutic agents from the nasal cavity to the brain.[2,3] Transport occurs along the olfactory pathway and likely involves extracellular bulk flow along perineuronal and/or perivascular channels, which allows for delivering drug directly to the brain parenchyma. Delivery along the extraneuronal pathway is likely not receptor-mediated and requires only minutes for a drug to reach the brain; whereas, delivery via an intraneuronal pathway along the primary olfactory sensory neurons involves axonal transport and requires several days for the drug to reach different areas of the brain.[38,39] It is possible that exosomes could be transported along the trigeminal nerve. Thorne *et al*.[40] proposed an extracellular pathway along trigeminal nerves for the transport of molecules from the nasal cavity to the brainstem and spinal cord. This was based on findings showing that after intranasal administration to rats of insulin-like growth factor-I, the molecule was observed in both rostral and caudal brain regions, consistent with entry points for the olfactory and trigeminal nerves, respectively. Although our imaging data did not show intranasal administered exosomes trafficking to caudal regions, it may be due to the lower sensitivity of the technology used in this study when compared with autoradiography used in Thorne *et al*. studies or size as we demonstrated is a factor that determines the route of trafficking.

Collectively, the delivery method demonstrated in this study may be particularly suited for potent therapeutics with adverse effects in the blood or in peripheral tissues, for therapeutic agents that are extensively bound to plasma proteins or degraded in the blood, or for oral drugs that lose their bioavailability or are not readily soluble in the gastrointestinal tract. The findings in this study should also shed a light on further study of effects of exosomes released from resident cells located in intranasal cavity on brain cells, in particular, brain immune cells. It is conceivable that exosomes released from local resident cells or exosomes translocated to the nasal cavity could play a role in brain immune tolerance, in particularly the innate immune response. This exosome-based delivery system potentially could be used to deliver other complementary and alternative medicines, like resveratrol, either alone or in combination with curcumin.

Although our findings demonstrated the potential for using exosomes as a novel, noninvasive delivery vehicle to target therapeutic drugs to the brain, more fundamental studies are required. Future studies are needed to determine the exact transportation route of exosomes from the olfactory region to the brain and their subsequent clearance. Additional research is also necessary to translate our results from animal models to clinical applications for humans, and to define the possible side effects of using exosomes as an intranasal delivery vehicle.

MATERIALS AND METHODS

Reagents. Curcumin, JSI-124 (cucurbitacin I) and LPS were purchased from Sigma-Aldrich (St Louis, MO) and dissolved in DMSO as stock solutions. A rabbit anti-Iba1 antibody that specifically recognizes microglial cells and macrophages was purchased from Wako Chemicals (Richmond, VA). Antibodies against total and phospho–Stat3 were purchased from Cell Signaling Technology (Danvers, MA). The following fluorescent dye-conjugated Abs were obtained from e-Bioscience (San Diego, CA): anti-CD11b, anti-CD45.2, anti-F4/80, anti-MHCII, and anti-IL-1β.

Cell lines. The mouse ($H\text{-}2^{b}$) glioblastoma cell line GL26 stably expressing the luciferase gene (GL26-Luc) and the BV2 microglial cell line were provided by Dr Behnam Badie (Beckman Research Institute of the City of Hope, Los Angeles, CA), and maintained in RPMI-1640 media supplemented with 10% heat-inactivated fetal bovine serum in a humidified CO_2 incubator at 37 °C. Cell lines including 3T3L1, 4T1, CT26, A20, and

EL-4 were purchased from ATCC and cultured according to the protocols provided (ATCC, Manassas, VA).

Preparation of exosomes and exosomal curcumin (Exo-cur) and JSI-124 (Exo-JSI124). All exosomes used in this study were prepared according to a previously described protocol.[14] Microparticles were prepared from supernatants of tumor cells grown to confluence (48 hours). The supernatants were sequentially centrifuged at 500*g* for 10 minutes and then at 1,200*g* for 30 minutes. Microparticles were then pelleted at 10,000*g* for 1 hour and washed once in PBS. The concentration of exosomes and microparticles was determined by analyzing protein concentration using the Bio-Rad protein quantitation assay kit (Bio-Rad Laboratories, Hercules, CA) with bovine serum albumin serving as a standard. Both Exo-cur and Exo-JSI124 were prepared by mixing curcumin or JSI124 with EL-4 exosomes in PBS. After incubation at 22 °C for 5 minutes, the mixture was subjected to sucrose gradient (8, 30, 45, and 60%, respectively) centrifugation for 1.5 hours at 36,000 r.p.m. Exo-cur or Exo-JSI124 was subsequently collected, washed, and resuspended in PBS. The concentration of curcumin or JSI124 in the complex was determined by high-performance liquid chromatography analysis.[14]

Animals. C57BL/6j mice (H-2^b) were purchased from the Jackson Laboratory (Bar Harbor, ME). Animals were housed in the animal facility at the University of Louisville per an Institutional Care and Use Committee-approved protocol.

Intranasal delivery of exosomes, Exo-cur, and Exo-JSI124 in mice. For intranasal administration of exosomes or exosome encapsulated drugs, C57BL/6j mice were anesthetized by I.P. injection of ketamine/xylazine (40 mg/5 mg/kg body weight) and placed in a supine position in an anesthesia chamber. PBS (2 µl) containing exosomes (2 µg/2 µl), or Exo-cur or Exo-JSI124 were administered intranasally as drops with a small pipette every 2 minutes into alternating sides of the nasal cavity for a total of 10 minutes. A total volume of 10 µl was delivered into the nasal cavity.

To determine the bioavailability of free curcumin and exosomal curcumin *in vivo*, two groups (five per group) of C57BL/6j mice were administered 1.5 nmol curcumin or Exo-cur intranasally. At 0, 3, 6, 12, and 24 hours, the brain was removed and curcumin was extracted from the tissue.[14] The concentration of curcumin in the extracts was determined by high-performance liquid chromatography as described.[14] The extracts from brain of naive mice without treatment either mixed with a known amount of curcumin or PBS were used as positive and negative controls, respectively. Also, formalin-fixed paraffin embedded nasal tissues were used for hematoxylin and eosin staining.

To monitor the trafficking of exosomes administered intranasally, exosomes were first labeled using an Odyssey fluorescent dye IRDye800 kit (LI-COR Biosciences, Lincoln, NE) or near-infrared lipophilic carbocyanine dye-dioctadecyl-tetramethylindotricarbocyanine iodide (Invitrogen, Carlsbad, CA) using a previously described method.[41] To localize EL-4 exosomes in brain tissue, the IRDye 800CW-or DIR-labeled EL-4 exosomes (10 µg/10 µl in PBS) were administered intranasally to C57BL/6j mice as described above. The mice were imaged over a 48-hour period using a prototype LI-COR imager (LI-COR Biosciences) for IRDye800-labeled exosomes or a Carestream Molecular Imaging system (Carestream Health, Woodbridge, CT) for DIR-dye labeled exosomes. For controls, mice (five per group) received nonlabeled EL-4 exosomes in PBS or free IRDye800 dye or DIR dye at the same concentration for IRDye800 or DIR dye-labeled exosomes.

Identifying the brain cells targeted by exosomes administered intranasally. Mice were administered intranasally PKH26 fluorescent dye-labeled exosomes (10 µg/mouse in 10 µl PBS) using the method described above. After intranasal administration, mice were transcardially perfused with PBS followed by a 4% paraformaldehyde solution at pH 7.4. Brain tissue was postfixed overnight in 4% paraformaldehyde and then cryopreserved in phosphate-buffered 30% sucrose. Brains were embedded in OCT compound (Tissue-Tek; Sakura, Torrance, CA) and kept at −20 °C overnight. Brain tissue sections were cut with a cryostat (30-µm thick) and the tissue sections stored at −20 °C. Immunofluorescent staining of microglial cells with rabbit anti-Iba1 antibody was carried out according to previously described procedures.[42] Tissues evaluated for the presence of Iba1 positive staining were assessed using a Zeiss LSM 510 confocal microscope equipped with a digital image analysis system (Pixera, San Diego, CA).

Brain tumor-bearing mice model. 2×10^4 GL26-Luc cells were intracranially injected per mouse using a method described previously.[43] In brief, using a Hamilton syringe (Hamilton Company, Reno, NV), 5×10^4 GL26-Luc cells in 2 µl PBS were stereotactically injected through an entry site at the bregma of anesthetized mice. Typically this procedure results in a 100% tumor take and a median survival time of ~28 days after tumor implantation. Tumor-bearing mice were treated intranasally for 12 consecutive days with daily doses of 12.5 pmol Exo-JSI24, JSI24 (12.5 pmol) or Exo-control in PBS or PBS-control. Treatment was initiated on day 3 after tumor cells were injected intracranially. The investigators treating the animals were fully blinded with regard to treatment. All mice were monitored every day and euthanized when they exhibited neurological symptoms indicative of impending death.

Monitoring the growth of injected tumor cells was accomplished by quantifying luciferase activity over a 15-day period post-tumor cell injection using a previously described method[44] with minor modifications. In brief, before the imaging session, the mice received an intraperitoneal injection of D-luciferine, a luciferase substrate (150 mg/kg; Xenogen, Alameda, CA) dissolved in PBS. The mice were then anesthetized with 2% isoflurane in 100% oxygen at a flow rate of 2 ml/min. Images were collected using a high-sensitivity CCD camera with wavelengths ranging from 300 to 600 nm with an exposure time for imaging of 2 minutes. Regions of interest were analyzed for luciferase signals using Living Image 2.50 software (Xenogen) and was reported in units of relative photon counts per second. The total photon count per minute (photons/minute) was calculated (five animals) using Living Image software. The effects of treatment versus nontreatment on brain tumor-bearing mice was determined by dividing the number of photons collected for treated mice by the number of photons collected for untreated mice at different imaging time points. Results were represented as pseudocolor images indicating light intensity (red and yellow being the most intense) that were superimposed over grayscale reference photographs.

LPS-induced brain inflammation. Bacterial LPS (2.5 mg/kg; Sigma-Aldrich) was injected intraperitoneally into C57BL/6j mice. Immediately after the LPS injection, mice were administered curcumin, Exo-cur (1.5 nmol in 10 µl PBS), or EL-4 exosomes equal to the amount in exosomal curcumin intranasally. EL-4 exosomes and PBS served as controls. Two hours after the treatments five mice from each group of mice (10 mice/group) were sacrificed and skulls of mice were removed, and the brains subsequently fixed for analysis of apoptosis induction using a method described previously.[45,46] The remaining mice (five mice per group) in each group were sacrificed and brain leukocytes were isolated. The percentage of activated microglial cells and apoptotic cells was determined by FACS analysis of $CD45.2^+IL\text{-}1\beta^+$ cells and $PI^+AnnexinV^+$ positive staining cells, respectively. Apoptosis in the brain was also evaluated by fluorescence using an *in situ* cell death detection kit (Roche, Indianapolis, IN) according to manufacturer's protocol. The expression of IL-1β in $CD45.2^+IL\text{-}1\beta^+$ cells was quantified by real-time PCR.[47]

***EAE induction and treatment with Exo-cur* in vivo.** EAE was induced in 6-week-old female C57BL/6 mice using a procedure described previously.[16] Briefly, mice were primed subcutaneously in the flanks with 150 µg of MOG35-55 peptide (Biosynthesis, Lewisville, TX) per animal. The peptide was emulsified in complete Freund's adjuvant containing 1 mg/ml of *Mycobacterium tuberculosis* H37RA (Difco, Detroit, MI). Two days later the mice were injected intraperitoneally with 500 ng of Pertussis toxin (Alexis,

San Diego, CA) in 100 µl of PBS. Mice (n = 10) were treated intranasally with daily doses of 1.5 nmol of Exo-cur, Cur-, or Exo-controls in PBS or PBS-control for 26 consecutive days. Treatment was initiated on day 4 after mice were primed with MOG35-55 peptide. The mice were scored as follows: 0, no detectable signs of EAE; 1, complete limp tail; 2, limp tail and hind limb weakness; 3, severe hind limb weakness; 4, complete bilateral hind limb paralysis; 5, total paralysis of both forelimbs and hind limbs or death.

Isolation of brain leukocytes. Brain leukocytes were isolated using a method described previously.[48] In brief, mice were sacrificed by CO_2 asphyxia and then perfused through the left cardiac ventricle with PBS. Brains were minced mechanically and cells from each brain were resuspended in 70% Percoll (Sigma-Aldrich), overlayed with 37% and 30% Percoll, and centrifuged at 500*g* for 20 minutes at 22 °C. Enriched brain leukocyte populations were recovered at the 70–37% Percoll interface. Quantification of subset populations present in the isolated cells was determined by antibody staining followed by FACS analysis[48] or western blot analysis of cell-specific proteins.

For FACS analysis of cell apoptosis, an Annexin-V fluorescein isothiocyanate/PI double-stain assay was performed according to the manufacturer's protocol (BioVision, Mountain View, CA). Briefly, leukocytes isolated from brain tissue were washed and resuspended in 500 µl of binding buffer containing 5 µl of Annexin-V fluorescein isothiocyanate and 5 µl of PI. The cells were incubated for 5 minutes in the dark at 22 °C. Analysis was done immediately using a flow cytometer.

Western blot. Western blots were done as previously described.[49] In brief, cells were lysed and proteins of lysed cells were separated on 10% polyacrylamide gels using SDS-PAGE. Separated proteins were transferred to nitrocellulose membranes. The western blot was carried out with the anti-Stat3 and anti-phospho-Stat3 antibodies (Cell Signaling) or anti-β-actin antibody as a control (Santa Cruz Biotechnology, Santa Cruz, CA).

Cytokine assay. Culture supernatants were assessed for the presence of mIL-IL-1β using an ELISA kit (eBioscience).

Quantitative real-time PCR. Relative quantification of select mRNA was performed using a CFX96 Realtime System (BioRad, Hercules, CA) and SsoFast evagreen supermixture (Bio-Rad Laboratories) according to the manufacturer's instructions. All primers were purchased from Eurofins MWG Operon (Huntsville, AL). Fold changes in mRNA expression between treatments and controls were determined by the ΔCT method.[50] Fluorescence threshold cycle (C_t) values were calculated using SDS 700 System Software (Bio-Rad). Results were normalized to the average C_t for the GAPDH and β-actin housekeeping genes run in the Quantitative real-time PCR. $\Delta\Delta C_t$ values were calculated to determine expression changes. Differences between groups were determined using a two sided Student's t-test and one-way ANOVA. Error bars on plots represent ± s.e., unless otherwise noted.

Statistical analysis. Survival data were analyzed by log rank test. Student's t-test was used for comparison of two samples with unequal variances. One-way ANOVA with Holm's *post hoc* test was used for comparing means of three or more variables.

ACKNOWLEDGMENTS

The authors thank Dr Behnam Badie (Beckman Research Institute of the City of Hope, Los Angeles, CA) for providing GL26-Luc and BV2 cell lines and Dr Aijian Qin (Yangzhou University, China) for technique assistance. This work was supported by grants from the Louisville Veterans Administration Medical Center (VAMC) Merit Review Grants (H.-G.Z.); the National Institutes of Health (NIH) (RO1CA137037, R01AT004294, R01CA116092, and R01CA107181); and a grant from the Susan G. Komen Breast Cancer Foundation. We thank Dr Jerald Ainsworth for editorial assistance.

REFERENCES

1. Potschka, H (2010). Targeting the brain–surmounting or bypassing the blood-brain barrier. *Handb Exp Pharmacol* 411–431.
2. Carvey, PM, Hendey, B and Monahan, AJ (2009). The blood-brain barrier in neurodegenerative disease: a rhetorical perspective. *J Neurochem* **111**: 291–314.
3. Gabathuler, R (2009). Blood-brain barrier transport of drugs for the treatment of brain diseases. *CNS Neurol Disord Drug Targets* **8**: 195–204.
4. Bidros, DS and Vogelbaum, MA (2009). Novel drug delivery strategies in neuro-oncology. *Neurotherapeutics* **6**: 539–546.
5. Yang, I, Han, SJ, Kaur, G, Crane, C and Parsa, AT (2010). The role of microglia in central nervous system immunity and glioma immunology. *J Clin Neurosci* **17**: 6–10.
6. Yadav, A and Collman, RG (2009). CNS inflammation and macrophage/microglial biology associated with HIV-1 infection. *J Neuroimmune Pharmacol* **4**: 430–447.
7. Choi, J and Koh, S (2008). Role of brain inflammation in epileptogenesis. *Yonsei Med J* **49**: 1–18.
8. Rock, RB and Peterson, PK (2006). Microglia as a pharmacological target in infectious and inflammatory diseases of the brain. *J Neuroimmune Pharmacol* **1**: 117–126.
9. Johnson, NJ, Hanson, LR and Frey, WH (2010). Trigeminal pathways deliver a low molecular weight drug from the nose to the brain and orofacial structures. *Mol Pharm* **7**: 884–893.
10. Garcia-Rodriguez, JC and Sosa-Teste, I (2009). The nasal route as a potential pathway for delivery of erythropoietin in the treatment of acute ischemic stroke in humans. *ScientificWorldJournal* **9**: 970–981.
11. Mistry, A, Stolnik, S and Illum, L (2009). Nanoparticles for direct nose-to-brain delivery of drugs. *Int J Pharm* **379**: 146–157.
12. Wu, H, Hu, K and Jiang, X (2008). From nose to brain: understanding transport capacity and transport rate of drugs. *Expert Opin Drug Deliv* **5**: 1159–1168.
13. Kastin, AJ and Pan, W (2006). Intranasal leptin: blood-brain barrier bypass (BBBB) for obesity? *Endocrinology* **147**: 2086–2087.
14. Sun, D, Zhuang, X, Xiang, X, Liu, Y, Zhang, S, Liu, C *et al.* (2010). A novel nanoparticle drug delivery system: the anti-inflammatory activity of curcumin is enhanced when encapsulated in exosomes. *Mol Ther* **18**: 1606–1614.
15. Théry, C, Ostrowski, M and Segura, E (2009). Membrane vesicles as conveyors of immune responses. *Nat Rev Immunol* **9**: 581–593.
16. Axtell, RC, de Jong, BA, Boniface, K, van der Voort, LF, Bhat, R, De Sarno, P *et al.* (2010). T helper type 1 and 17 cells determine efficacy of interferon-β in multiple sclerosis and experimental encephalomyelitis. *Nat Med* **16**: 406–412.
17. Gräler, MH (2010). Targeting sphingosine 1-phosphate (S1P) levels and S1P receptor functions for therapeutic immune interventions. *Cell Physiol Biochem* **26**: 79–86.
18. Shelton, RC and Miller, AH (2010). Eating ourselves to death (and despair): the contribution of adiposity and inflammation to depression. *Prog Neurobiol* **91**: 275–299.
19. Scott, KF, Sajinovic, M, Hein, J, Nixdorf, S, Galettis, P, Liauw, W *et al.* (2010). Emerging roles for phospholipase A2 enzymes in cancer. *Biochimie* **92**: 601–610.
20. Choi, JW, Herr, DR, Noguchi, K, Yung, YC, Lee, CW, Mutoh, T *et al.* (2010). LPA receptors: subtypes and biological actions. *Annu Rev Pharmacol Toxicol* **50**: 157–186.
21. Berquin, IM, Edwards, IJ and Chen, YQ (2008). Multi-targeted therapy of cancer by omega-3 fatty acids. *Cancer Lett* **269**: 363–377.
22. Murakami, A and Ohigashi, H (2007). Targeting NOX, INOS and COX-2 in inflammatory cells: chemoprevention using food phytochemicals. *Int J Cancer* **121**: 2357–2363.
23. Harizi, H and Gualde, N (2006). Pivotal role of PGE2 and IL-10 in the cross-regulation of dendritic cell-derived inflammatory mediators. *Cell Mol Immunol* **3**: 271–277.
24. Kühn, H and O'Donnell, VB (2006). Inflammation and immune regulation by 12/15-lipoxygenases. *Prog Lipid Res* **45**: 334–356.
25. Frey, AB (2006). Myeloid suppressor cells regulate the adaptive immune response to cancer. *J Clin Invest* **116**: 2587–2590.
26. Huang, B, Pan, PY, Li, Q, Sato, AI, Levy, DE, Bromberg, J *et al.* (2006). Gr-1$^+$CD115$^+$ immature myeloid suppressor cells mediate the development of tumor-induced T regulatory cells and T-cell anergy in tumor-bearing host. *Cancer Res* **66**: 1123–1131.
27. Kusmartsev, S and Gabrilovich, DI (2002). Immature myeloid cells and cancer-associated immune suppression. *Cancer Immunol Immunother* **51**: 293–298.
28. Kusmartsev, S and Gabrilovich, DI (2003). Inhibition of myeloid cell differentiation in cancer: the role of reactive oxygen species. *J Leukoc Biol* **74**: 186–196.
29. Fitzner, D, Schnaars, M, van Rossum, D, Krishnamoorthy, G, Dibaj, P, Bakhti, M *et al.* (2011). Selective transfer of exosomes from oligodendrocytes to microglia by macropinocytosis. *J Cell Sci* **124**(Pt 3): 447–458.
30. Patil, BS, Jayaprakasha, GK, Chidambara Murthy, KN and Vikram, A (2009). Bioactive compounds: historical perspectives, opportunities, and challenges. *J Agric Food Chem* **57**: 8142–8160.
31. Ravindran, J, Prasad, S and Aggarwal, BB (2009). Curcumin and cancer cells: how many ways can curry kill tumor cells selectively? *AAPS J* **11**: 495–510.
32. Anand, P, Thomas, SG, Kunnumakkara, AB, Sundaram, C, Harikumar, KB, Sung, B *et al.* (2008). Biological activities of curcumin and its analogues (Congeners) made by man and Mother Nature. *Biochem Pharmacol* **76**: 1590–1611.
33. Campbell, FC and Collett, GP (2005). Chemopreventive properties of curcumin. *Future Oncol* **1**: 405–414.
34. Thomasset, SC, Berry, DP, Garcea, G, Marczylo, T, Steward, WP and Gescher, AJ (2007). Dietary polyphenolic phytochemicals–promising cancer chemopreventive agents in humans? A review of their clinical properties. *Int J Cancer* **120**: 451–458.
35. Tomita, M, Matsuda, T, Kawakami, H, Uchihara, JN, Okudaira, T, Masuda, M *et al.* (2006). Curcumin targets Akt cell survival signaling pathway in HTLV-I-infected T-cell lines. *Cancer Sci* **97**: 322–327.
36. Wright, TI, Spencer, JM and Flowers, FP (2006). Chemoprevention of nonmelanoma skin cancer. *J Am Acad Dermatol* **54**: 933–46; quiz 947.
37. Xie, L, Li, XK, Funeshima-Fuji, N, Kimura, H, Matsumoto, Y, Isaka, Y *et al.* (2009). Amelioration of experimental autoimmune encephalomyelitis by curcumin

treatment through inhibition of IL-17 production. *Int Immunopharmacol* **9**: 575–581.
38. Thorne, RG, Emory, CR, Ala, TA and Frey, WH 2nd (1995). Quantitative analysis of the olfactory pathway for drug delivery to the brain. *Brain Res* **692**: 278–282.
39. Balin, BJ, Broadwell, RD, Salcman, M and el-Kalliny, M (1986). Avenues for entry of peripherally administered protein to the central nervous system in mouse, rat, and squirrel monkey. *J Comp Neurol* **251**: 260–280.
40. Thorne, RG, Pronk, GJ, Padmanabhan, V and Frey, WH 2nd (2004). Delivery of insulin-like growth factor-I to the rat brain and spinal cord along olfactory and trigeminal pathways following intranasal administration. *Neuroscience* **127**: 481–496.
41. Wang, GJ, Liu, Y, Qin, A, Shah, SV, Deng, ZB, Xiang, X *et al.* (2008). Thymus exosomes-like particles induce regulatory T cells. *J Immunol* **181**: 5242–5248.
42. Wang, J, Li, C, Liu, Y, Mei, W, Yu, S, Liu, C *et al.* (2006). JAB1 determines the response of rheumatoid arthritis synovial fibroblasts to tumor necrosis factor-α. *Am J Pathol* **169**: 889–902.
43. Alizadeh, D, Zhang, L, Brown, CE, Farrukh, O, Jensen, MC and Badie, B (2010). Induction of anti-glioma natural killer cell response following multiple low-dose intracerebral CpG therapy. *Clin Cancer Res* **16**: 3399–3408.
44. Liu, C, Yu, S, Kappes, J, Wang, J, Grizzle, WE, Zinn, KR *et al.* (2007). Expansion of spleen myeloid suppressor cells represses NK cell cytotoxicity in tumor-bearing host. *Blood* **109**: 4336–4342.
45. Zhang, HG, Huang, N, Liu, D, Bilbao, L, Zhang, X, Yang, P *et al.* (2000). Gene therapy that inhibits nuclear translocation of nuclear factor κB results in tumor necrosis factor α-induced apoptosis of human synovial fibroblasts. *Arthritis Rheum* **43**: 1094–1105.
46. Liu, Z, Xu, X, Hsu, HC, Tousson, A, Yang, PA, Wu, Q *et al.* (2003). CII-DC-AdTRAIL cell gene therapy inhibits infiltration of CII-reactive T cells and CII-induced arthritis. *J Clin Invest* **112**: 1332–1341.
47. Zhang, HG, Hyde, K, Page, GP, Brand, JP, Zhou, J, Yu, S *et al.* (2004). Novel tumor necrosis factor α-regulated genes in rheumatoid arthritis. *Arthritis Rheum* **50**: 420–431.
48. Deng, ZB, Poliakov, A, Hardy, RW, Clements, R, Liu, C, Liu, Y *et al.* (2009). Adipose tissue exosome-like vesicles mediate activation of macrophage-induced insulin resistance. *Diabetes* **58**: 2498–2505.
49. Liu, Y, Xiang, X, Zhuang, X, Zhang, S, Liu, C, Cheng, Z *et al.* (2010). Contribution of MyD88 to the tumor exosome-mediated induction of myeloid derived suppressor cells. *Am J Pathol* **176**: 2490–2499.
50. Zhao, S and Fernald, RD (2005). Comprehensive algorithm for quantitative real-time polymerase chain reaction. *J Comput Biol* **12**: 1047–1064.